Theoretical investigation of stoichiometric lithium monoboride

H. Rosner* and W. E. Pickett
Department of Physics, University of California, Davis, California 95616
(Received 5 September 2002; published 27 February 2003)

Structural energies around two recently reported diffraction results of nominally stoichiometric LiB samples have been investigated using full potential electronic structure methods. It is found that one of the reported structures is unstable to large relaxations of the hexagonal lattice constants. Calculations of a pseudodiamond structure and other B-chain derived structures indicate that this ambient pressure, stoichiometric lithium-monoboride system is indeed characterized by strongly double-bonded B chains. However, the structure is subject to very low-energy motions of Li atoms along the *c* axis, and also to relative displacements of B chains along the *c* direction. The B chains themselves are robust, with the boron bond-stretching mode at 138 meV. Although the deformation potential for this phonon mode is substantial, nevertheless the electron-phonon coupling is rather small and superconductivity can be expected at best only at low temperature. The lowest-energy geometry within this class of structures is identified, but due to only tiny differences in total energy, samples are likely to contain several types of structural imperfection as suggested by diffraction data.

DOI: 10.1103/PhysRevB.67.054104 PACS number(s): 64.30.+t, 71.20.Gj

I. INTRODUCTION

Since the unexpected discovery of high-temperature phonon-coupled superconductivity in MgB_2,[1] interest in simple compounds of boron and light elements has undergone a Renaissance. Doping on both the Mg and B sites has proven unproductive in raising critical temperature (T_c). This finding has led both theorists and experimentalists to the (re)investigation of structurally related compounds.[2]

A promising candidate, $Li_{1-x}BC$, has been suggested as possibly an even better superconductor than MgB_2. LiBC itself is isostructural (except for minor complexities) and isovalent to MgB_2, but is semiconducting due to the B-C modulation in the graphene layer. Predictions, based on first-principles density-functional calculations and buttressed by the similarity of LiBC to MgB_2, indicate $Li_{1-x}BC$ should be a similar, or even higher-T_c, superconductor than MgB_2 for $x \geqslant 0.25$. Attempts at experimental verification are underway.[3,4] A related layered borocarbide MgB_2C_2 has been suggested as a possible superconductor if hole doped,[5,6] but it is not so closely related to MgB_2 and no indication of its electron-phonon coupling strength has yet appeared.

The lithium-boron system with a composition ratio Li:B near to 1:1 has attracted interest as an anode material for battery applications. While there is no reason to suspect it could also be a good superconductor, there are structural reasons to suspect that there are strong B-B bonding states in a metallic compound, which is the central feature of MgB_2 that sets it apart from the previous "high-T_c" intermetallic compounds.[7] There were earlier reports of a LiB compound, reported as strong, refractory, and porous.[8] Reports followed on a compound with stoichiometry of Li_5B_4,[9] with a rhombohedral crystal structure proposed by Wang *et al.*[10] The stoichiometry Li_7B_6 was obtained by Dalleck *et al.*[11] and reproduced by James and Devries.[12] In these studies there was no indication as to why a specific stoichiometry should be favored, and the Li mobility suggests that several stoichiometries may be possible. Mair *et al.* have reported on Li_3B_{14} and discussed work reporting other compositions.[13]

The recent x-ray-diffraction (XRD) analysis of multiphase samples of nominally stoichiometric LiB by Liu *et al.*[14] pointed to a relatively simple hexagonal structure (described below). However, the small electronic charge on the Li atom makes its position difficult to determine from powder diffraction. Moreover, the extreme reactivity of the elements and large differences in their melting temperatures pose difficulties in producing high quality, single phase samples. At about the same time, Wörle and Nesper performed x-ray and neutron-diffraction analyses of single phase samples that indicated a similar structure of the B chain, but the diffraction intensity was hard to fit to a well-defined crystal structure.[15]

This stoichiometric LiB system appears, however, to be ideal for the application of *ab initio* band-structure techniques to help determine the crystal structure by comparing energies for different lattice constants, internal parameters (atomic positions),[16,17] and even different structures.[18] This is the path we have taken, and we will describe our investigations chronologically. For the lowest-energy structure, the contribution of the B bond-stretching modes to possible superconductivity is estimated.

II. CALCULATIONAL METHODS

A full potential nonorthogonal local-orbital scheme[19] within the local-density approximation (LDA) was used to obtain accurate band structures and the total energies that we report. A full potential method is necessary when optimizing the hexagonal c/a ratio and for comparing different structures. In the scalar relativistic calculations we used the exchange and correlation potentials of Perdew and Zunger.[20] Li($1s$, $2s$, $2p$, $3d$) and B ($2s$, $2p$, $3d$) states, respectively, were chosen as the basis set. The lower-lying B $1s$ states were treated as core states. The Li $2p$ and $3d$ states as well as the B $3d$ states were taken into account to increase the completeness of the basis set. The inclusion of the Li $1s$ states in the valence states was necessary to account for non-negligible core-core overlaps. The spatial extension of the basis orbitals, controlled by a confining potential[21] (r/r_0),[4]

was optimized to minimize the total energy.

Since the energy differences between some of the structures that we study are very small, dense k-point meshes ($50\times50\times50$ in the full Brillouin zone) have been used for all structures. Special care, and convergence tests, have also been carried out for the local-orbital basis sets, and for the Fourier representation of the potential.

III. CRYSTAL STRUCTURE

A. Experimentally reported structure: α-LiB

Liu *et al.* obtained the best refinement of x-ray data for the hexagonal space group No. 194 ($P6_3/mmc$) with lattice constants $a=4.022$ Å, $c=2.796$ Å.[14] In the unit cell with two formula units (f.u.), B and Li occupy the Wyckoff positions $2b$ (0,0,1/4) and $2c$ (1/3,2/3,1/4), respectively. The structure is shown in the top panel of Fig. 1, and consists of hexagonal sheets of B, with Li lying at interstitial sites within the B layers in alternating positions along the c axis. The structure can also be considered from the viewpoint of a hexagonal array of B chains oriented along the c axis, and this viewpoint will become more useful below. We will refer to this structure as α-LiB, from which we begin our investigation of structures.

The first step in exploring configuration space was to relax the volume with respect to the reported value of $c/a=0.695$ for α-LiB. The equation of state is shown in Fig. 2, with the relaxed volume found to be *nearly 20% larger*[22] than what was reported, a remarkably large discrepancy. Subsequent relaxation of the c/a ratio produced the value 0.77 at the optimum volume (which is itself now much closer to the reported value). For the optimized lattice constants, the in-plane value $a=4.019$ Å is remarkably close to the experimental report,[14] whereas the calculated hexagonal axis $c=3.102$ Å exceeds the reported value[14] by more than 10%.

The band structure of the relaxed α-LiB system is shown in Fig. 3. The valence bands consist of two types of states. Filled B sp_z σ bands lie in the -4 to -10 eV region. They disperse by less than 0.5 eV perpendicular to the chain orientation (note the $A-L-H-A$ and $\Gamma-M-K-\Gamma$ directions in Fig. 3), so all of their dispersion arises from simple nearest-neighbor hopping along the chain, with hopping amplitude $t_\sigma\approx10$ eV/4$=$2.5 eV. The density of states (DOS), shown in Fig. 4, indeed displays (somewhat broadened) indications of one-dimensional van Hove singularities near the corresponding band edges at -10 eV and -4 eV.

The other type of states are the chain π-bonding B p_x,p_y states. They disperse along the chain similarly to the σ bands, but in addition interchain coupling results in k_x,k_y dispersion of about 3 eV (again, see $A-L-H-A$). Li character is minor in the valence bands. The Li-related charge has mainly an overlap character and an ionic picture is well justified. A van Hove singularity lies precisely at the Fermi level (E_F), associated with the π band that grazes E_F at the H point of the zone. The occupation of bonding σ bands by two electrons per LiB unit leaves two to occupy the π bands. Due to the dispersion of the π bands in all directions, the Fermi surfaces have no strong one-dimensional or two-dimensional features. We return to the Fermi surfaces later.

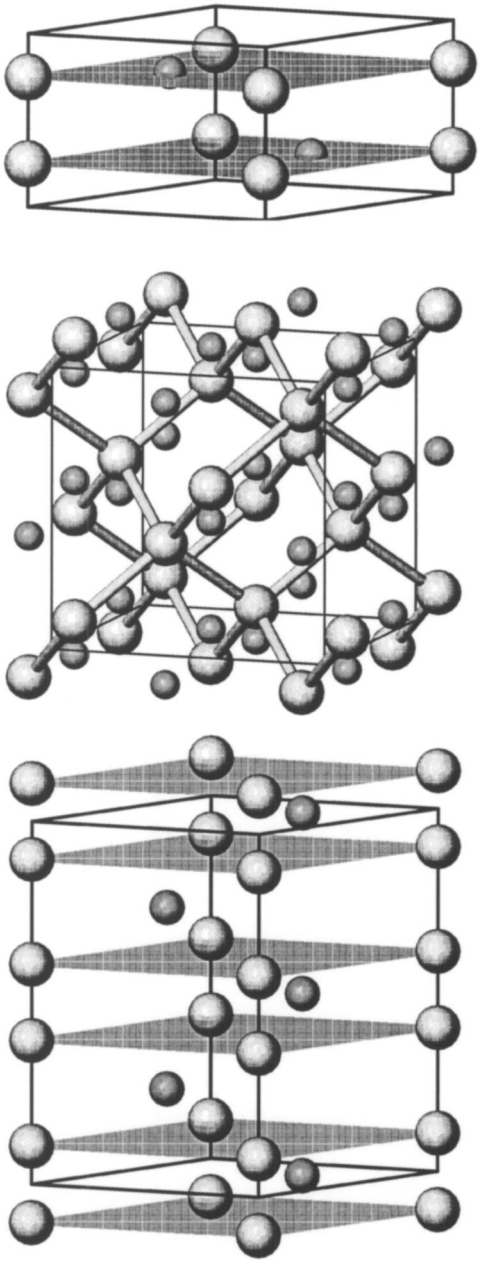

FIG. 1. Different structure types for LiB considered in this paper. The top panel illustrates one unit cell of the structure (α-LiB) reported by Liu *et al.* (Ref. 14). The large, lightly shaded spheres are boron and the smaller darker spheres are lithium atoms, respectively. The middle panel illustrates one unit cube of the pseudodiamond structure (c-LiB), with sticks denoting B-B bonds. A doubled unit cell of the "intercalated" β-LiB structure type is shown at bottom. The different B-B distances along the chains correspond to the bond-stretching mode discussed in Sec. III D.

In the upper panel of Fig. 4, a comparison of the densities of states for the experimental and for the optimized lattice constants shows considerable differences. The value of the DOS at E_F, a key ingredient for all thermodynamic properties, differs by more than a factor of 2 for the two lattice parameter sets. The reason is an overestimate of the B-B bonding along the c direction for the very short experimental

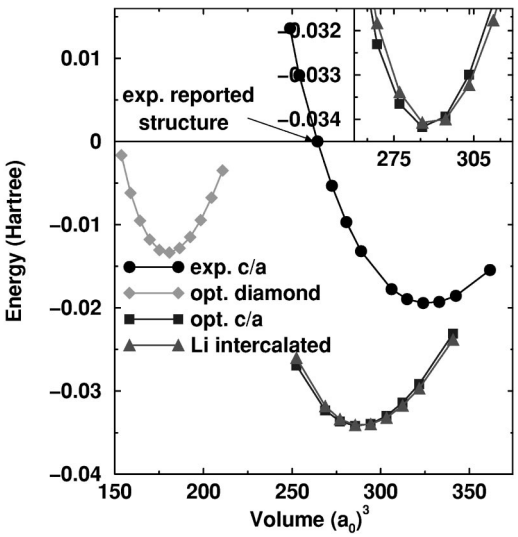

FIG. 2. Calculated relative total energy versus volume for several of the LiB structures considered in this paper. The energy of the reported structure (Ref. 14) is taken as the reference ($E=0$). Long curve: relaxation of the volume for the reported structure and c/a ratio. Left-hand curve: equation of state for the pseudodiamond structure of *c*-LiB. Bottom curves: energy after full structural optimization in the reported space group, and the ''intercalated'' β-LiB structure in which the Li atoms lie between the B layers rather than within the layers. The energy difference between these last two structures, shown with a finer energy scale in the inset at the upper right corner, is quite small (see text).

c parameter. This short B-B bond moves the bonding σ states downwards by almost 1 eV (see Fig. 4) and enlarges the dispersion of the π-bonding B p_x, p_y states along this direction. As a result, the van Hove singularity at the Fermi level is moved away from it, causing the drastic change in the DOS value at E_F.

The gain in energy due to this full relaxation is 0.017 hartree$\sim$0.5 eV/f.u. Since the diffraction pattern of this structure should not be confused with that of the very different c/a that was reported, the inevitable conclusion was that alternative structures needed to be considered.

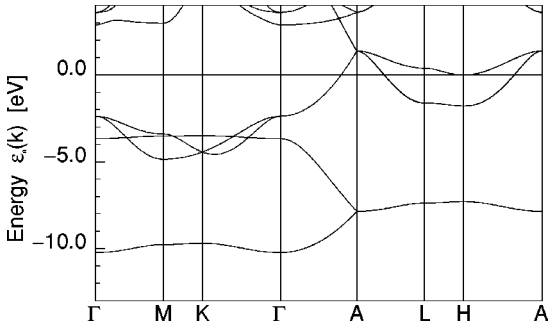

FIG. 3. Band structure of LiB for the optimized *c* and *a* values of the experimentally reported space group, corresponding to the density of states in Fig. 4. The Fermi level is at zero energy. The dispersion along the $\Gamma-A$ line arises from σ-bonding states (-4 to -10 eV) and π-bonding (crossing the Fermi level) states. The dispersion along $A-L-H-A$ reflects coupling between the B chains, which is only $\sim$0.5 eV for the σ states, but is about 3 eV for the π states and crucial for determing the Fermi surfaces and density of states in the region of the Fermi level.

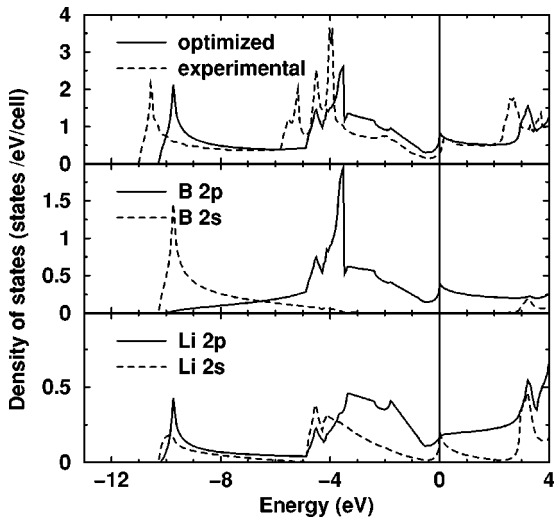

FIG. 4. Total as well as partial densities of states of LiB for the optimized values of *c* and *a*, in the experimentally reported space group (the top panel of Fig. 1). The Fermi level, taken as the zero of energy, lies just at a van Hove singularity.

B. Pseudodiamond structure type: c-LiB

Because of the tendency of boron to form covalent networks and the ''isoelectronicity'' of stoichiometric combinations of LiB to C (assuming considerable ionicity), we investigated a possible ''pseudodiamond'' structure[23] in the cubic space group No. 227 ($Fd3m$) with B and Li occupying the Wyckoff positions 8*a* (1/8,1/8,1/8) and 8*b* (3/8,3/8,3/8), respectively. This fictitious ''pseudodiamond'' structure, which we refer to as (cubic) *c*-LiB and which is shown in the middle panel of Fig. 1, has B atoms lying on the C sites of the diamond lattice, and Li atoms lying at the interstitial holes [which form an identical diamond sublattice displaced from the B one by ($a/2,a/2,a/2$) along a B-B bond direction].

The resulting band structure (see Fig. 5) and density of states (see Fig. 6) of *c*-LiB is indeed quite diamondlike qualitatively, with a calculated direct energy gap at Γ of 1.5 eV.

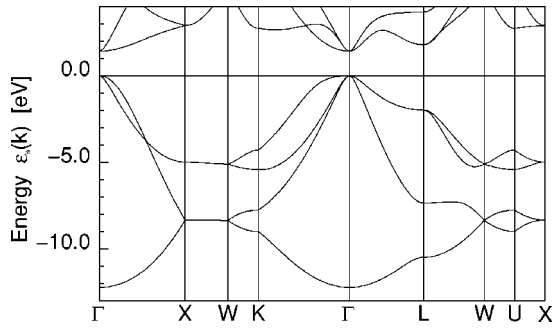

FIG. 5. Band structure corresponding to the ''pseudodiamond'' density of states of LiB shown in Fig. 6. The zero of energy is put at the bottom of the energy gap.

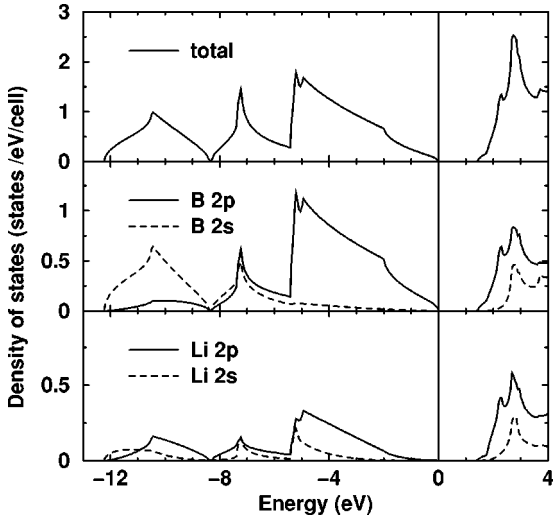

FIG. 6. Total as well as partial densities of states of LiB for the optimized ''pseudodiamond'' structure type (compare middle panel, Fig. 1). The zero of energy is placed at the bottom of the band gap. The total DOS bears a considerable similarity to that of diamond.

The corresponding calculated (indirect) gap value in diamond is 4.2 eV, about a 30% underestimate of the observed gap. The valence bands of *c*-LiB are of very strong B $2s,2p$ origin, with appreciable Li character appearing only in the conduction bands, so the valence states of LiB are analogous to those of diamond. Thus, electronically, *c*-LiB indeed resembles diamond, with B sp^3 bonds standing in for the C sp^3 bonds in diamond. The structure can be expected to be mechanically stable, although we have not made any specific calculations to verify this. The optimized lattice constant is 4.74 Å, compared to 3.57 Å (Ref. 24) for diamond and 5.43 Å (Ref. 25) for Si, respectively. The calculated valence bandwidth is about 12 eV, very close to that of Si, and much smaller than the 21-eV bandwidth of diamond, reflecting the considerably shorter and stronger bonding in diamond.

In this structure, the cubic lattice constant is the single structural parameter, hence the structure is simple to optimize. The equation of state is shown in Fig. 2 beside the energies discussed previously. This pseudodiamond structure is lower than that of the reported structure[14] by 0.2 eV/f.u., but it is still 0.3-eV higher than the fully relaxed structure obtained in the previous subsection. Thus while this crystal structure may indeed be mechanically stable, it is only metastable, and in fact is at least 0.6-eV/f.u. above the most stable structure. These energy differences lead to an important realization: while the single bonds in pseudodiamond *c*-LiB may be strong and quite favorable energetically, the double-bonded B-B chain is substantially stronger, having considerably greater binding energy. This fact suggests retaining the B chains in the structure, while investigating other structural changes.

C. "Li-intercalated" structure type: β-LiB

To begin to investigate the influence of different Li arrangements on the energy and electronic structure, we considered what might be pictured as a ''Li-intercalated'' rearrangement of the experimentally reported structure. Compared to the α-LiB structure[14] the Li position is shifted relative to the hexagonal B planes along the *c* axis by $c/4$, placing the Li atoms in between those planes. This change retains the hexagonal space group No. 194 ($P6_3/mmc$), but now B and Li occupy the Wyckoff positions $2a$ (0,0,0) and $2c$ (1/3,2/3,1/4), respectively. This structure, which we refer to as β-LiB, is pictured in the bottom panel of Fig. 1.

The resulting optimized structure has $c=3.118$ Å, $a=4.031$ Å, quite close to that of relaxed α-LiB reference structure discussed in Sec. III A. The total energy is quite close, as shown in Fig. 2. It differs by about 0.5 meV/f.u. (see Table I), which is at the border of computational accuracy for the comparison of different structures.

D. Stability to dimerization

The (metallic) quasi-one-dimensional boron chains along the *c* direction raise the possibility of lattice instability with respect to dimerization, well known for polyacetylene,[26] which is isovalent but is a buckled chain rather than a linear chain. We calculated the total energy for several B dimerization amplitudes, starting from the Li-intercalated structure type doubled along the hexagonal axis.[27] The dimerization reduces the symmetry, leading to the hexagonal space group No. 188 ($P\bar{6}c2$) with two inequivalent Li sites at $2c$ (1/3,2/3,0) and $2f$ (2/3,1/3,1/4) and a fourfold B position at $4g$ $(0,0,z)$. The structure is shown in the bottom panel of Fig. 1. The dimerization amplitude is determined by $0.125-z$.

TABLE I. Calculated lattice parameters and total energies for the different investigated LiB structures. The energy of the experimentally reported reference structure (Ref. 14) (first row) containing 2 f.u. is set to zero. The lattice parameters of the δ-LiB structure have been reexpressed in pseudohexagonal notation for easy comparison with other numbers in the column; the lattice constants for the *Pmma* setup are given in parentheses. For details see text.

Structure	Space group	Lattice parameters (Å)	Wyckoff positions	Total energy (m hartree)
α-LiB (experiment)	$P6_3/mmc$	$a=4.022$, $c=2.796$	B $(2b)$, Li $(2c)$	0.0
α-LiB (optimized)	$P6_3/mmc$	$a=4.019$, $c=3.102$	B $(2b)$, Li $(2c)$	-34.12
c-LiB	$Fd\bar{3}m$	$a=4.74$	B $(8a)$, Li $(8b)$	-13.38
β-LiB	$P6_3/mmc$	$a=4.031$, $c=3.118$	B $(2a)$, Li $(2c)$	-34.08
δ-LiB	*Pmma*	$a'(b)=4.019$, $c'(a)=3.102$	B $(2a)$, $(2f)$: $z=\frac{1}{2}$,	-34.04
(Staggered)		$b'(c=\sqrt{3}b)=6.961$	Li $(2e)$:$z=\frac{1}{3}$, $(2f)$: $z=\frac{5}{6}$	

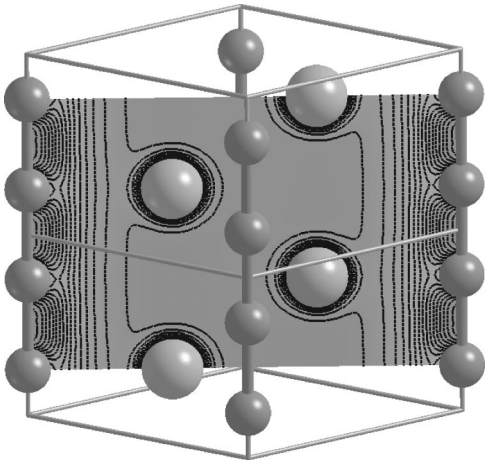

FIG. 7. Contour plot of the calculated charge density for the α-LiB structure for a layer perpendicular to [110] through the origin of the unit cell. Shown are two unit cells: the large spheres are the Li atoms and the small spheres are the B atoms with the strong covalent bonds indicated.

Our calculated total energies for dimerization amplitudes up to 0.05 Å show no evidence for a structural instability, consistent with the calculated Fermi surfaces which bear no resemblance to one-dimensional planes. An energy versus dimerization plot can be fitted parabolically with very small deviations only, resulting in a calculated phonon frequency of 138 meV in the harmonic approximation, reflecting very strong B-B double bonds.

E. Staggered B chains: δ-LiB

According to the XRD and neutron-diffraction analyses of Wörle and Nesper,[15] the best refinement of their samples was obtained in terms of boron chains that individually are rigid, but whose B positions are uncorrelated along the *c* axis. We have modeled this lack of correlation by an orthorhombic supercell with the *Pmma* (No. 51) space group, containing two crystallographically independent B chains which lie along the *a* axis in this setting. For the modeling of the chain disorder, we fix one sublattice with B atoms at $2a$ (0,0,0) and Li sites at $2e$ $(1/4,0,z=1/3)$ and $2f$ $(1/4,1/2,z=5/6)$, respectively. In one case the second B chain has its B positions at $2d$ (0,0,1/2), corresponding to the original α-LiB structure and corresponding to an ''in-phase'' arrangement. A second structure, which we call δ-LiB, has the B sites in the second chain at the $2f$ (1/4,1/2,1/2) position, corresponding to a rigid shift of the chain by half of the B-B separation, producing a pair of chains in the structure with a ''staggered'' arrangement.

We obtained a practically negligible difference in total energy (2 meV/f.u.) between the structures, the staggered arrangement being possibly slightly higher in energy. Differences in the band structure are also nearly invisible in a band plot and in the DOS.

In order to better understand the microscopic reason for the uncorrelated boron chains, we calculated the charge density for a layer perpendicular to [110] through the origin of the unit cell (see Fig. 7). Very remarkably, the charge-density isocontours around the B chains along the *c* direction are almost parallel by a distance of about 1 Å from the chain axis. The lack of appreciable correlation of the B-chain density is consistent with the lack of correlation of B positions between neighboring chains.

F. Incommensurabilities and pressure effects

The results for energetics and densities in the preceeding subsections provide a very instructive explanation of the conclusion of Wörle and Nesper that the B chains are oriented along the *c* axis but otherwise are uncorrelated. From our calculated total energies we find that various *z*-axis displacements of B chains relative to each other cost almost no energy, and perhaps at room temperature the chains can even slide against each other, or perhaps more precisely, can slide with respect to the underlying Li sublattice which seems to be well established. The density plot shown in Fig. 7, which would be very similar in the α-LiB and β-LiB structures, can be compared directly with the electron density observed by XRD (see Fig. 4 in Ref. 15). The superposition of calculated charge densities for different B arrangements leads to a picture which is remarkably similar to the XRD pattern ''integrating'' over all the different B positions.

Wörle and Nesper in fact infer an incommensurate periodicity of the Li sublattice and the B-chain periodicity along the *c* axis. The Li-Li layer separation is $c/2=1.43$ Å, while the average B-B separation is inferred to be 1.59 Å. This difference leads to an atomic B:Li ratio of $\sim 9{:}10$ if the Li sublattice is fully occupied. It is not so straightforward for us to test this conclusion with our total-energy calculations.[28] This picture is supported by a kink in x-ray and neutron background scattering reported in Ref. 15. Therein, the observed kink could be simulated by a model containing 400 B chains randomly shifted against each other in the *c* direction. Though Wörle and Nesper[15] suggested the possibility of alternating single and triple bonds (1.78 Å and 1.40 Å) rather than uniform double bonds (1.59 Å), their analysis could not distinguish them. The calculated Fermi surfaces are not sufficiently one dimensional to induce a Peierls distortion. Our calculated B-B bond length of 1.55 Å and the stability against dimerization strongly favor the latter picture.

These structural considerations have not made use of the *c*-LiB phase that we suggested. This cubic phase may, however, have some experimental relevance. Performing the Maxwell common-tangent construction in Fig. 2 between the optimal structure and that of *c*-LiB, one finds that under pressure LiB should transform into *c*-LiB at $P=-(dE/dV)_{common}=0.9$ GPa, unless some phase we have not considered intervenes. If pressure synthesis of *c*-LiB were to be successful, its similarity to silicon would be interesting to study.

IV. SUPERCONDUCTIVITY

Because of the similarity of one of the basic features responsible for the high T_c in MgB_2, the strong metallic bonds at the Fermi energy, we discuss in this section the possibility of MgB_2-type superconductivity in more detail. The similari-

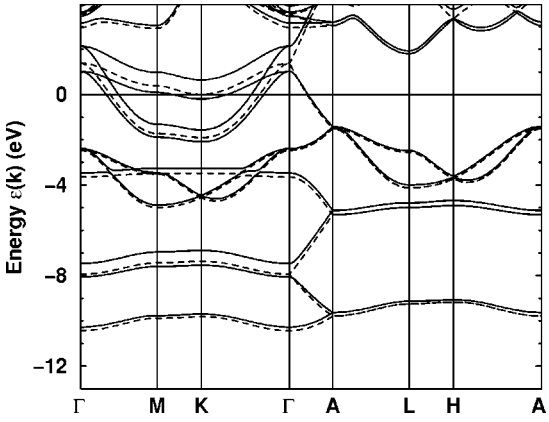

FIG. 8. Band structure for the dimerized (full lines) β-LiB (see lower panel of Fig. 1). For comparison, the undistorted band structure in the same unit cell is drawn with dashed lines.

ties in fact extend further: covalent B-B bonding together with positive ions in a metallic system, and all atoms have small mass.

To estimate the electron-phonon coupling strength λ we use an approach that revealed that the B-B bond-stretching modes were driving the superconductivity in MgB_2.[7] We have calculated the deformation potential $\mathcal{D}$ for this bond-stretching mode from the band shifts and splittings of originally degenerate bands that are shown in Fig. 8. The splitting is especially large for the π bands crossing the Fermi level along the hexagonal plane (recall that the σ bonds are filled and therefore inactive). From the splitting Δ of these bands at the Γ point we obtain $\mathcal{D}=\Delta/(2u)\approx 8.3$ eV/Å where u is the displacement of each B atom. $\mathcal{D}$ is remarkably large for a metal, although with only $\sim 65\%$ of its value of about 13 eV in MgB_2.[7] Following the approach of Ref. 7 to estimate T_c for MgB_2 we use the expressions provided by Khan and Allen[29] applied to the bond-stretching related coupling:

$$\lambda = 2N(\varepsilon_F)\left[\frac{1}{M\omega^2}\right]\left|\sum_{j=1,2}\hat{\epsilon}_j\vec{\mathcal{D}}_j\right|^2 + \lambda_{other}$$
$$= \lambda_{stretch} + \lambda_{other}. \quad (1)$$

In this expression, only the single bond-stretching branch is considered explicitly, and the deformation potential and frequency are assumed to be independent of wave vector Q; all other modes lead to the other, possibly minor, contribution λ_{other}. The sum over j runs over the two moving B atoms of the bond-stretching mode. With $N(0)=0.37$ states/eV (per spin) and the calculated phonon frequency $\omega=138$ meV, Eq. (1) results in $\lambda_{stretch}\sim 0.25$. Applying the Allen-Dynes[30] or McMillan equation with a Coulomb pseudopotential $\mu^*\sim 0.1$, we find critical temperatures T_c of the order of 0.1 K. This leads to the conclusion that the very high phonon frequency $\omega=138$ meV of the bond-stretching mode, entering Eq. (1) in the denominator and making this denominator five times larger than in MgB_2, disfavors superconductivity despite the considerable deformation potential. In retrospect, it is clear that the high bond-stretching frequency is consistent with (even indicative of) weak coupling, otherwise this frequency would be renormalized downward considerably, as it is in MgB_2 compared with AlB_2, and as it is in the $Li_{1-x}BC$ system.[31]

Although other phonon modes certainly will enlarge the overall electron-phonon coupling, these contributions are probably small because of the weak interaction between the chains discussed in Sec. III E (concerning all the related phonons) and the minor Li character at the Fermi level (concerning the Li-related phonons). Therefore, we expect superconductivity in LiB only at very low temperatures if it becomes superconducting at all.

V. DISCUSSION AND SUMMARY

In the present paper, we have discussed various crystal structures for the stoichiometric LiB system. Although the experimentally reported parameters for the α-LiB structure type result in a much higher total energy than the optimized fictitious diamondlike c-LiB compound, several fully relaxed hexagonal structure types are still deeper in energy, but all of them show extremely close total-energy values. Taking into account that all the measurements were done at room temperature, we would not expect any of the considered hexagonal phases to be considerably favored against another. From our simulation for the staggered B chains in δ-LiB we conclude that the rigid boron chains can slide against each other with almost no cost of energy. Together with the calculated stability against dimerization this leads us to a picture of a fixed Li sublattice hosting rigid but uncorrelated B chains formed by B-B double bonds.

The strong B-B double bond leads to a relatively large deformation potential, about two-thirds of the corresponding deformation potential in MgB_2. However, the high phonon frequency $\omega=138$ meV of this bond-stretching mode results in only a small electron-phonon coupling λ for this mode, if our simple estimate is reliable. We conclude that MgB_2-type superconductivity cannot be expected for the hexagonal LiB phases under consideration.

ACKNOWLEDGMENTS

We thank Yuri Grin for fruitful discussions and a critical reading of the manuscript. This work was supported by the National Science Foundation, Grant No. DMR-0114818 (W.E.P.), and by the Deutscher Akademischer Austauschdienst (H.R.).

*Present address: Max Planck Institute for Chemical Physics of Solids, Noethnitzer Str. 40, D-01187 Dresden, Germany.

[1] J. Nagamatsu, N. Hakagawa, T. Muranaka, Y. Zenitani, and J. Akimitsu, Nature (London) **410**, 63 (2001).

[2] H. Rosner, A. Kitaigorodsky, and W.E. Pickett, Phys. Rev. Lett. **88**, 127001 (2002).

[3] J. Hlinka, I. Gregora, A.V. Pronin, and A. Loidl, cond-mat/0207683 (unpublished).

[4] A. Bharathi, S. Jemima Balaselvi, M. Premila, T.N. Sairam, G.L.N. Reddy, C.S. Sundar, and Y. Hariharan, cond-mat/0207448 (unpublished).
[5] P. Ravindran, P. Vajeeston, R. Vidya, A. Kjekshus, and H. Fjellvag, Phys. Rev. B **64**, 224509 (2001).
[6] H. Harima, Physica C **378**, 18 (2002).
[7] J.M. An and W.E. Pickett, Phys. Rev. Lett. **86**, 4366 (2001).
[8] F. E. Wang, in Ref. 14.
[9] F.E. Wang, Metall. Trans. A **10A**, 343 (1979).
[10] F.E. Wang, M.A. Mitchell, R.A. Sutula, and J.R. Holden, J. Less-Common Met. **61**, 237 (1978).
[11] S. Dalleck, D.W. Ernst, and B.F. Larick, J. Electrochem. Soc. **126**, 866 (1979).
[12] S.D. James and L.E. Devries, J. Electrochem. Soc. **123**, 321 (1976).
[13] G. Mair, R. Nesper, and H.G. von Schnering, J. Solid State Chem. **75**, 30 (1988).
[14] Z. Liu, X. Qu, B. Huang, and Z. Li, J. Alloys Compd. **311**, 256 (2000).
[15] M. Wörle and R. Nesper, Angew. Chem. Int. Ed. Engl. **39**, 2349 (2000).
[16] D. Singh and W.E. Pickett, Nature (London) **374**, 682 (1995).
[17] H. Rosner, S.-L. Drechsler, K. Koepernik, I. Opahle, and H. Eschrig, in *Rare Earth Transition Metal Borocarbides* (*Nitrides*): *Superconducting, Magnetic and Normal State Properties* (Kluwer Academic Publishers, Dordrecht, 2001).
[18] P. Soderlind, O. Eriksson, B. Johansson, J.M. Wills, and A.M. Boring, Nature (London) **374**, 524 (1995).
[19] K. Koepernik and H. Eschrig, Phys. Rev. B **59**, 1743 (1999).
[20] J.P. Perdew and A. Zunger, Phys. Rev. B **23**, 5048 (1981).
[21] H. Eschrig, *Optimized LCAO Method and the Electronic Structure of Extended Systems* (Springer, Berlin, 1989).
[22] Usually, the cell volume estimated by LDA calculations is smaller than the experimentally observed volume due to the well-known overbinding in this method.
[23] This structure type is realized in the isovalent NaTl compound.
[24] T. Hom, W. Kiszenick, and B. Post, J. Appl. Crystallogr. **8**, 457 (1975).
[25] C.R. Hubbard, H.E. Swanson, and F.A. Mauer, J. Appl. Crystallogr. **8**, 45 (1975).
[26] M.J. Rice, A.R. Bishop, and D.K. Campbell, Phys. Rev. Lett. **23**, 2136 (1983).
[27] For the intercalated β LiB, the bond B-B stretching phonon creates two inequivalent Li sites and, therefore, a doubling of the unit cell along the crystallographic *c* direction.
[28] A comparison of different crystal structures with respect to stability based on total-energy calculations can only be done for a fixed stoichiometry.
[29] F.S. Khan and P.B. Allen, Phys. Rev. B **29**, 3341 (1984).
[30] P.B. Allen and R.C. Dynes, Phys. Rev. B **12**, 905 (1975).
[31] J.M. An, S.Y. Savrasov, H. Rosner, and W.E. Pickett, Phys. Rev. B **66**, 220502 (2002).